On the Importance of Electric Currents Flowing directly into the Mould during an ESR Process

A. Kharicha[1], W. Schützenhöfer[2], A. Ludwig[1], R. Tanzer[2], M.Wu[1]
[1] University of Leoben, Franz-Joseph strasse, 8. 8700 Leoben, AUSTRIA
[2] Böhler Edelstahl GmbH & Co KG, Kapfenberg, AUSTRIA

ABSTRACT: In the present paper a numerical model is developed to predict the exact electric current paths in the slag region of an ESR process. The model solves the momentum and energy equations. The solidification of the slag at the mould is modeled with an enthalpy-porosity approach. The magnitude of the Joule heating and the Lorentz force are derived from the computed electric current lines. The localization where the Joule heating occurs controls the temperature distribution. The electric current distribution is in turn influenced by the temperature field through the temperature dependant electric conductivity. With this numerical tool the electric current paths are exactly computed by choosing the less resistive way to the liquid pool, or to the mould. For a given electric intensity the model predicts the power generated by the system and the solidified slag thickness at the mould. The model is validated by comparing its results with experiments on a small scale ESR process.

1. INTRODUCTION

The Electro-Slag-Remelting (ESR) is an advanced technology for the production of high quality materials e.g. hot work tool steels or nickel base alloys. An alternating current (AC) is passed from a conventionally melted and cast solid electrode through a layer of molten slag to the baseplate (Fig. 1). Because of the electrical resistivity of the slag, Joule heating is generated and the slag transfers this energy to ingot and mould surfaces and to the melting electrode tip. The molten metal produced in the form of droplets passes through the slag and feeds a liquid pool from where directional solidification takes place. The slag and the ingot are contained in a water cooled copper mould. As also the baseplate is water cooled, a heat flow regime is imposed that gives controlled solidification, and this results in improved structure characteristic of ESR ingots.

Proper modeling of this melting process depends on the ability of the model to predict the right electric current patterns in the system which controls the magnitude and the location where the Joule heating occurs. One of the most important parameter is the electrical conductivity of the slag. This parameter increases strongly in magnitude with increasing temperature, so the slag is much more conducting in its liquid phase than in its solid phase. It is generally assumed [1-6] that due to its very low electric conductivity, the solidified slag layer insulates perfectly the slag from the copper mould. Depending on the chemical composition of the slag, the ratio between liquid and solid slag-skin electric conductivity is of the order of *10-100.* This ratio depends strongly on the actual temperature of the slag-skin layer. Most of simulations found in literature use the hypothesis of perfectly isolated mould which has also the advantage to simplify considerably the formulation of the electromagnetic boundary conditions at the mould. The fact that in most of the industrial ESR devices the mould and the baseplate are in contact brings the possibility that the current, instead of crossing the slag thickness, goes directly to the mould. There it can then flow to the baseplate without resistance. Based on the values given in Tab. 1, the thickness of the solidified slag is small (e_S *~0.1-5 mm*), and the radial resistance of this layer ($\sim e_S / \sigma_S$) is still smaller or of the same order of magnitude as the vertical resistance of liquid slag ($\sim H / \sigma_1$). Kharicha et al [7] have theoretically considered the influence of mould currents on the hydrodynamic interaction between a layer of slag and a layer of steel when a vertical current is imposed. The shape of the slag/steel interface was found to be considerably modified when the current was not allowed to enter the mould. More recently, the model of A.D. Patel [8] accounts for the mould currents by artificially directing a part (20 %) of the total current towards the mould. Nevertheless, this model was not able to predict the exact proportion represented by the mould current over the total current.

In the present paper a numerical model is presented where no insulation hypothesis is made. The current is left free to choose the less resistive way to the liquid pool or to the

mould. The model is applied to a slag region of a small scale ESR process where the pool/slag interface is assumed to be flat. The flow, temperature and turbulence fields are solved assuming the axisymmetricity of the system. The solidification field is resolved with the help of an enthalpy-porosity method. To illustrate the capability of the model, two simulations are performed, the first using the classical insulation hypothesis, the second without this hypothesis. The results of these two simulations are then compared with experimental data.

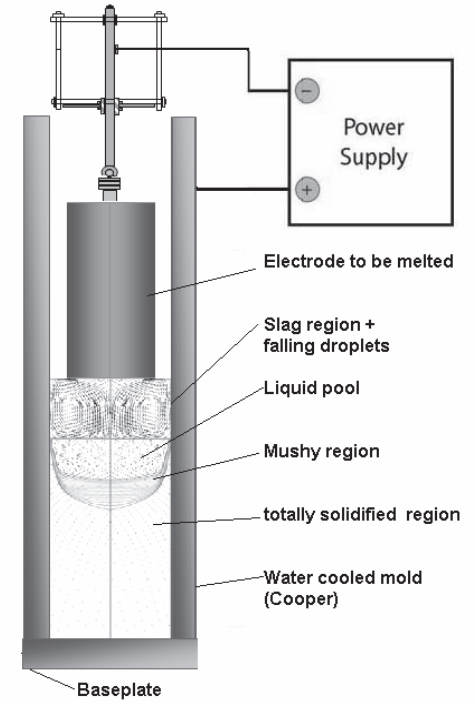

Fig. 1: Schematic view of the ESR system

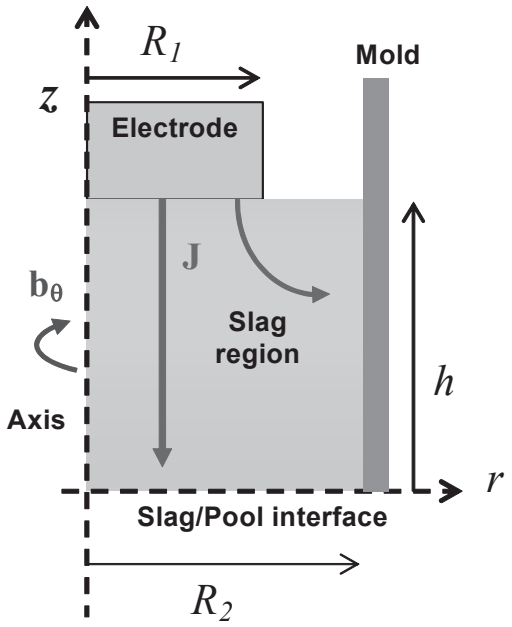

Fig. 2: Calculation domain: the slag region

2. MODEL DESCRIPTION

An electrode is put in contact with a cylindrical container filled with a layer of liquid slag (Fig. 2). The properties of the slag e.g. the density (ρ), dynamical viscosity (μ), and electrical conductivity (σ) are considered to be temperature dependant. The magnetic permeability (μ_0) is the same everywhere and equal to the vacuum magnetic permeability. Table 1 lists typical average physical properties of the slag, the geometry and the operating conditions used for the present simulations.

2.1 Flow Dynamics and Turbulence

The buoyant fluid flow is modelled with the Navier-Stokes equation according to

$$\rho\frac{D\vec{u}}{Dt} = -\nabla p - \rho\ \vec{g}\beta(T - T_{\mathrm{Re}f}) + \nabla(\mu_T(\nabla\vec{u} + \nabla\vec{u}^T)) + S + \mu_0\ \mathrm{Re}(\frac{1}{2}\vec{j}\times\tilde{H}_{\theta\,Conjugate}) . \qquad (1)$$

Here p represents the pressure and g the gravitational acceleration. The effect of turbulent mixing is taken into account through the effective viscosity μ_T. The Boussinesq approximation is used for determining the buoyancy force. S is the momentum sink at the mushy zone, see next section for more details.The last term on the right hand side of Eq. (1) represents the Lorentz force. The no-slip boundary condition is imposed at all boundaries except at the exposed slag surface and at liquid pool surface where a free slip condition is used. In the RNG k-ε turbulence model the time-averaged velocity field is solved together with equations for the transport of turbulent kinetic energy, k, and its dissipation, ε.

2.2 Energy Equation

The temperature distribution is governed by the energy conservation equation:

$$\rho\ c_p \frac{DT}{Dt} = \nabla(k_T(\nabla T)) + \mathrm{Re}(\frac{1}{2\sigma}\tilde{\vec{j}} \times \tilde{\vec{j}}_{\theta\ Conjugate}) - \rho L \frac{D\lambda}{Dt} \quad (2)$$

Where L is the latent heat, and k_T the turbulent thermal conductivity. A linear relation between temperature and liquid fraction $\lambda = (T - T_{Solidus})/(T_{Liquidus} - T_{solidus})$ was used. Once the liquid fraction is known, the momentum sink in Eq. (1) is then calculated according to: $S = -A \cdot (1-\lambda)^2 \cdot \vec{u} / \lambda^3$, where A is the mushy zone constant, equal to 10^4. The temperature is set to the steel liquidus temperature at the electrode. At the exposed slag surface heat is lost through radiation. The Influence of the falling steel droplets are not taken into account in the present investigation. A constant value of heat transfer coefficient is applied over the entire height of the slag. To avoid contact between the liquid slag and the mould, the value of the heat transfer coefficient is progressively increased until the liquid fraction becomes strictly equal to zero all over the mould surface.

2.3 Electromagnetics

The imposed vertical current is distributed over the entire domain according to the distribution of the slag electric conductivity. For sinusoidal AC field, we can express the induced magnetic field in complex notation: $H_\theta = \tilde{H}_\theta e^{i\omega t}$ .The complex amplitude $\tilde{H}_\theta$ is a function of the position, and ω is the angular frequency. The equation to be solved can be expressed as:

$$\frac{\partial}{\partial r}(\frac{1}{\sigma\ \mu_0 \cdot r}\frac{\partial}{\partial r}(r\tilde{H}_\theta)) + \frac{\partial}{\partial z}(\frac{1}{\sigma\ \mu_0 \cdot r}\frac{\partial}{\partial z}(r\tilde{H}_\theta)) = i\omega\tilde{H}_\theta \quad (3)$$

The resolution is performed for both real and imaginary parts of this equation. Due to the very high difference between the electrical conductivity between the electrode and the slag, the radial current is assumed to be zero at the electrode. The same condition is used at the slag/pool interface: $\partial\tilde{H}_\theta/\partial z = 0$. Applying the Ampere's law at the exposed slag surface gives the condition on the magnetic flux: $\tilde{H}_\theta(r) = I_0/2\pi$, where I_o denotes the amplitude of the total current, and *r* the radial distance to the rotating axis. For the simulation which assumes that the current does not enter the mould, the boundary condition is $\tilde{H}_\theta(r) = I_0/2\pi R_2$. For the second case the mold is considered as perfectly conducting wall, It can be shown that the boundary condition at the mould fulfils : $\partial\tilde{H}_\theta/\partial r = -\tilde{H}_\theta/R_2$. Once the magnetic flux is known, the electric current density is obtained through: $\tilde{\vec{j}} = \vec{\nabla} \times (\tilde{H}_\theta \vec{e}_\theta)$

3. RESULTS

The two cases presented below were tested by comparing the results with experimental data [9]. The comparisons concern the total power generated in the slag region which is electrically measured during the process. Due to its characteristic microstructure, the thickness of the solidified slag layer at the mould has been measured after total solidification of the slag region. The slag temperature has been measured with a thermocouple from the free surface to the mid-height of the slag.

3.1 Insulating Mould

In this case the computed current distribution is in accordance with the classical view of the ESR process. The current density is very high, and the main driving force for the slag flow is the Lorentz force. The later creates an anti-clockwise motion of the mean flow. The location where the Joule heating is at its maximum, is at the electrode extremity. The temperature of the slag is about 2700 K (Fig. 3). The solidified slag layer shows a minimum thickness at the bottom slag/pool interface and a maximum thickness at the top slag surface (Fig. 4b). The maximum and minimum are separated by a large area with a nearly constant thickness. The bottom minimum is created by the hot flow impingement at the mould. In contact with the cold mould, the slag flow becomes cooler during its elevation. The

accumulation of cold slag at the top corner explains the thick slag layer. Compared to experimental data, the present configuration leads to sensible different slag thickness and different total Joule heat release (Tab. 2).

3.2 Conducting Mould

In this case the current is free to choose the less resistive way to reach either the liquid pool or the mould. In Fig. 3 it can be seen that 90 % of the current is able to cross the solid slag layer to enter the mould. This proportion is far higher than what expected. The consequence is that in the present configuration the solid slag layer has nearly no insulating effect. The region where the Joule heating occurs is extended from the electrode extremity to the vicinity of the mould. The key to understand the electric current configuration is the temperature distribution. Hot slag being more conducting than cold slag, the current leaving the electrode is directed towards the hottest region. It can be observed that the main characteristics (direction and magnitude) of the flow is similar to that found with the insulating hypothesis.

The solidified slag layer shows now two minimums, a first at the slag/pool interface, and a second at the level of the free slag surface. This top minimum is the direct consequence of the near wall Joule heating which is able to heat up the rising cold slag flow. The flow pattern is very similar to the one from the case with insulating mould. The bottom minimum is also created by the hot flow impingement at the mould. The slag temperature is about 400K lower than in the insulating mould case, the reason lies on the fact that the power generated by the system is three times smaller (Tab. 2). A smaller slag temperature explains also the larger solidified slag thickness.

The present case shows definitively the closest results to experimental data (Tab. 2). The computed power generated in the slag and the solidified slag thickness, are of the same order than that found in experiments.

4. CONLCUSION

The electric current path lines for an ESR process were computed according to the electric conductivity distribution in the slag domain including a thin solidified slag layer at the slag/mould interface. It has been shown that the resistance of the solid slag layer is not high enough to prevent the current to enter the mould. If an insulating assumption is used, the total heat generated in the slag region was found to be 140% higher than that really generated during the process. The computations with a conducting solid slag layer gave results only 10 % smaller than in the experiments. It should also be noticed that the results obtained for the solid slag thickness, explain why often during ESR processes there are two peaks in the heat fluxes measured at the mould. The bottom peak is due to the hot slag flow impingement onto the mould, the peak at the top is due to the occurrence of the near wall Joule heating created by the current entering the mould. The non existence of the top peaks (in some ESR processes) could be a sign that only a little or no current enter directly the mould. In fact the results of the model are extremely dependant on the actual variation of the electric conductivity with temperature. To stop the current, the solidified slag layer must be at least 1000 times more resistive than the slag at liquid state. It is clear that other slags and other geometries (fill ratio) can give totally different results. Nevertheless, through this work it is clear that the assumption that the electric current cannot cross the solidified slag layer must be used with extreme care.

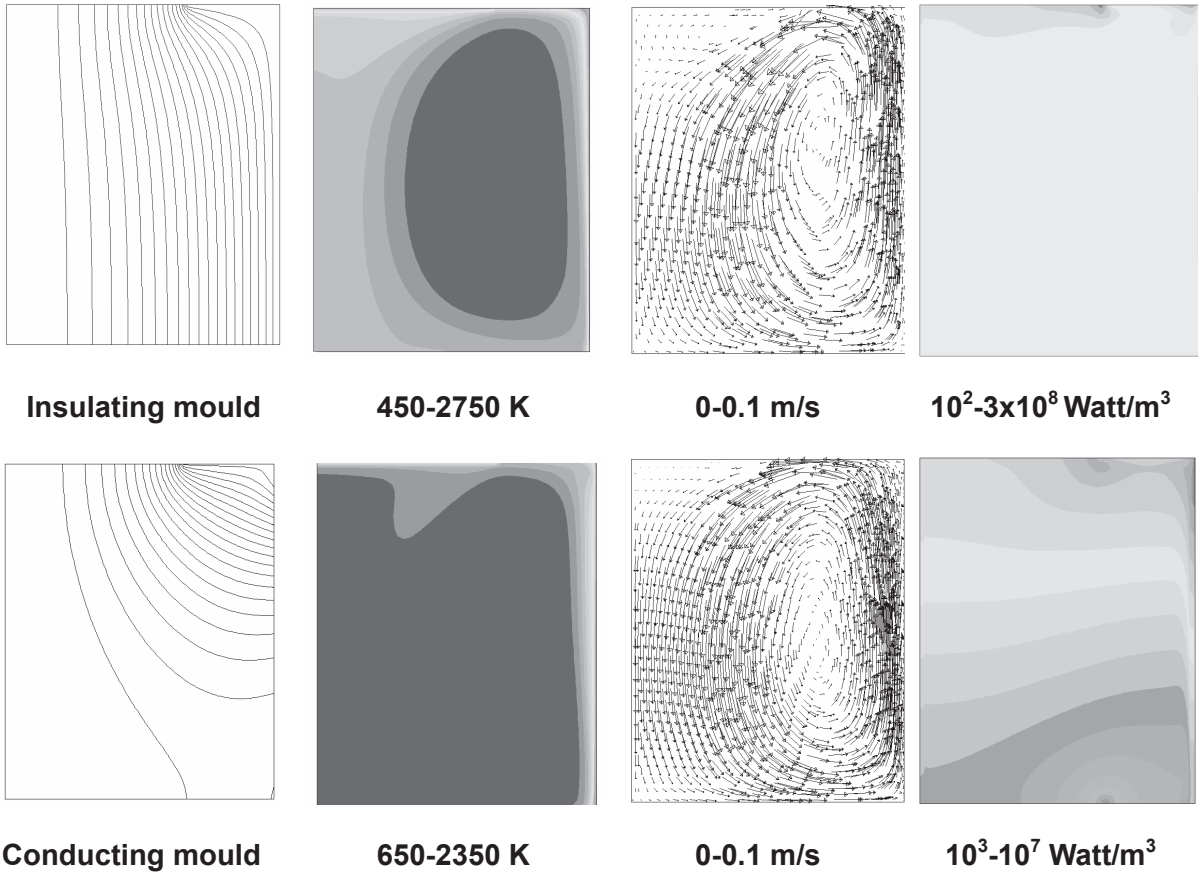

Fig. 3: Electric currents, temperature, flow and Joule heating in the slag region for the two cases.

Slag	
Density	2800 kg/m^3
Viscosity	0.04 kg/ms
Liquidus temperature	1450 K
Solidus temperature	1300 K
Latent heat of fusion	1.5*10^4 J/kg
Specific heat, liquid	1255 J/kgK
Thermal expan. coefficient	2.5 x 10^{-4} K^{-1}
Electric conductivity, 1000 K	1.0x10^1 $(\Omega m)^{-1}$
Electric conductivity, 1870 K	1.2x10^2 $(\Omega m)^{-1}$
Thermal conductivity, 2000 K	6.0 W/mK
Thermal conductivity, 750 K	0.5 W/mK

Geometry	
Slag height (h)	125 mm
Electrode diameter (2xR_1)	130 mm
Ingot diameter (2xR_2)	200 mm
Operating condition (experimental ESR)	
Electric current	5 Hz 4.5 kA
Slag emissivity	0.8

Tab. 1: Physical properties and operating conditions used for the present study.

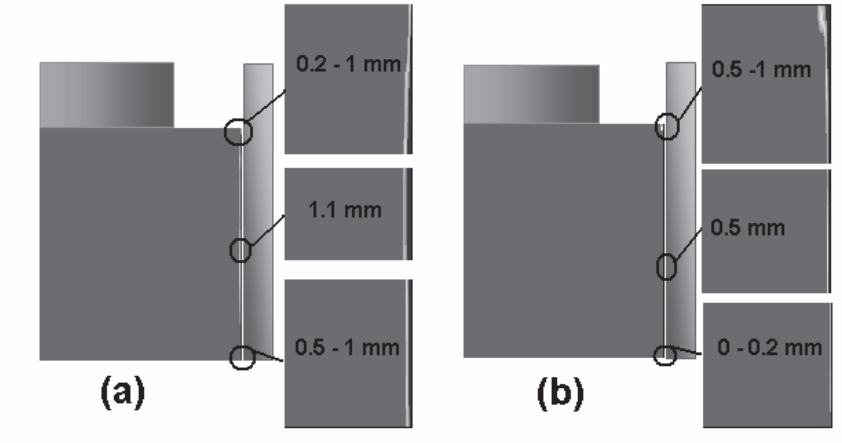

Fig 4. Solidified slag thickness along the mould in the free current case (a) and the insulated mould case (b).

	Total power dissipation	Averaged solid slag thickness	Maximum temperature	Heat transfer coefficient used (from slag to water)
Experimental	185 kW	~1 mm	2300 K	?
Numerical with insulating mould	450 kW	0.5 mm	2800 K	25 000 W/m^2/K
Numerical with conducting mould	165 kW	1.2 mm	2400 K	4500 W/m^2/K

Tab. 2: Some experimental and numerical results

5. ACKNOWLEDGEMENTS

This project is funded by the “European Research Fund for Coal and Steel“ under Contract No. RFS-CR-04027 for which the authors kindly acknowledge.

6. REFERENCES

[1] M. Choudhary and J. Szekely, Metall. Trans. B, Vol. 11B, (1980), p.439-453.

[2] M. Choudhary and J. Szekely. Ironmaking & Steelmaking, Vol. 5, (1981), p.225-232.

[3] B. Hernandez-Morales and A. Mitchell, Ironmaking & steelmaking, Vol. 26 No. 6 (1999), p.423-438

[4] A. H. Dilawari and J. Szekely, Metall. Trans. B, Vol 8B, (1997), p.227-236.

[5] K. Tacke, K. Schwerdfeger, C. Zellerfeld, Melting of the ESR electrode. Arch. Eisenhüttenwes. 52, No 4, (1981), p.137-142.

[6] A. Mitchell and S. Joshi, Metall. Trans., Vol. 2, (1971), p.449-445

[7] A. Kharicha, A. Ludwig and M. Wu. Mater. Sci. Eng. Vol. A 413-414 (2005), p.129-134.

[8] A.D. Patel. Proceedings LMPC, Santa Fe, USA (2005) p.18-21

[9] W. Schützenhöfer, G. Reiter, R. Tanzer, H. Scholz, R. Sorci, F. Arcobello-Varlese and A. Carosi: Proceedings LMPC, Nancy France, Sept 2-5, 2007, to be published.